Appl. Phys. 16, 121—138 (1978)

Applied Physics

Collective and Single-Electron Interactions of Electron Beams with Electromagnetic Waves, and Free-Electron Lasers*

A. Gover
California Institute of Technology, Pasadena CA 91125, USA, and Tel-Aviv University, Ramat-Aviv, Israel

A. Yariv
California Institute of Technology, Pasadena, CA 91125, USA

Received 22 October 1976/Accepted 25 October 1977/Corrected proofs received 14 March 1978

Abstract. The field of radiation emission from electron beams is reviewed with special reference to work related to free-electron lasers. Different schemes of interaction in periodic structures, electromagnetic slow-wave structures, and in transverse confining force are distinguished. Various effects and devices such as traveling wave amplifiers, Smith-Purcell radiators, Cerenkov and bremsstrahlung-free electron lasers, cyclotron resonance masers, coherent bremsstrahlung and channeling radiation are discussed and the differences and relations among them are explained. A simple comprehensive model is developed to describe electron-beam interaction with an electromagnetic wave in periodic electromagnetic structures. The model is general enough to describe both collective and single-electron modes of interaction and quantum mechanical, classical and Fermi degenerate regimes. Simplified expressions are developed for the gain by stimulated emission of radiation and for gain conditions of the Smith-Purcell-Cerenkov type free-electron lasers under conditions of very thin electron beams and infinite interaction length.

PACS: 32, 42.60, 84

The present paper is concerned with the problem of electromagnetic wave interactions with electron beams and free electron lasers. Using a comprehensive physical point of view we will discuss the different regimes of interactions (single-electron and collective interaction) and explain the common features and the differences between various effects and devices like Smith-Purcell radiation, traveling wave amplifiers, magnetic bremsstrahlung, free-electron lasers, Cerenkov lasers, cyclotron resonance masers, channeling radiation and coherent bremsstrahlung.

While we will first review briefly the present research on free-electron lasers and discuss the above listed effects by means of a general qualitative model, we will consequently embark in greater detail on the analysis of the special case of interactions in slow electromagnetic wave structures (Cerenkov-Smith-Purcell free electron lasers). The simple model used, instructively delineates the transitions between the single-electron and collective interaction regimes and between conventional laser theory and electron tube theories of the electron beam-electromagnetic wave interactions.

In a quantum mechanical model the first-order interaction of a free electron with a radiation field involves a radiative transition of the electron from an initial state $|i\rangle$ to a final state $|f\rangle$. The transition rate is proportional to the square of the matrix element of the interaction Hamiltonian which to first order in the vector potential A is

$$\langle f|\mathscr{H}'|i\rangle = -\frac{e}{2m}\langle f|p\cdot A(r,t)+A(r,t)\cdot p|i\rangle\,. \tag{1}$$

* This research is supported by the Air Force Office of Scientific Research under contract AFOSR-76-2933

0340-3793/78/0016/0121/$03.60

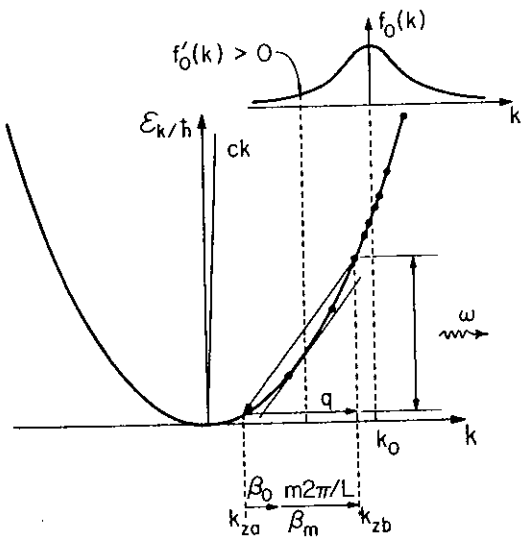

Fig. 1. Schematic one dimensional illustration of free-electron radiative transition. $f_0(k)$ is the electron beam distribution function

If we consider free-electron wave functions and a plane electromagnetic wave

$$|i\rangle = \frac{1}{V}\exp(\mathrm{i}\boldsymbol{k}_i\cdot\boldsymbol{r} - \mathrm{i}\mathscr{E}_i t/\hbar)$$

$$|f\rangle = \frac{1}{V}\exp(\mathrm{i}\boldsymbol{k}_f\cdot\boldsymbol{r} - \mathrm{i}\mathscr{E}_f t/\hbar) \tag{2}$$

$$A(\boldsymbol{r},t) = A(\boldsymbol{q},\omega)\exp(\mathrm{i}\boldsymbol{q}\boldsymbol{r} - \mathrm{i}\omega t)$$

we find that the matrix element in (1) is nonvanishing only if both conditions of momentum and energy conservation are satisfied.

$$\mathscr{E}_i - \mathscr{E}_f = \hbar\omega \tag{3}$$

$$\boldsymbol{k}_i - \boldsymbol{k}_f = \boldsymbol{q} \tag{4}$$

so radiative electronic transitions can take place only between electronic states which satisfy (3) and (4).

Radiative transitions can take place from the higher electronic state to a lower one, emitting a photon, or from a lower state to a higher one absorbing a photon. Figure 1 is a one-dimensional schematic description of radiative emission. An electronic transition takes place from state k_{zb} to state k_{za}, emitting a photon with energy

$$\mathscr{E}_{k_{zb}} - \mathscr{E}_{k_{za}} = \hbar\omega \tag{5}$$

and wave number

$$k_{zb} - k_{za} = q, \tag{6}$$

where we assumed that the electromagnetic field propagates in the z direction.

If the electron population at $k_z = k_{zb}$ is higher than the population at $k_z = k_{za}$

$$f_0(k_{zb}) > f_0(k_{za}), \tag{7}$$

then there will be more radiative emission transitions than radiative absorption, and we will observe net amplification of an electromagnetic wave due to stimulated transitions of the interacting electrons at states $k_z = k_{zb}$ and $k_z = k_{za}$ (see Fig. 1). This gain condition, referred to as "the population inversion condition" is completely equivalent to the gain condition in conventional lasers. Here the population inversion is attained by simply accelerating the electrons so that the peak of their distribution k_0 will be shifted from zero (see Fig. 1). If $k_0 = 0$ (as in thermal equilibrium of the electron gas) only stimulated absorption can take place. If population inversion obtains it is straightforward to show from (3) and (4) that the group velocity of the electron beam exceeds the phase velocity of the electromagnetic wave

$$v_g > v_{ph}, \tag{8}$$

where $v_g \equiv 1/\hbar\partial/\partial k_z \mathscr{E}_{k_z}|_{k_z = k_0}$ and $v_{ph} \equiv \omega/q$. This gain condition will be referred to as the "Cerenkov condition". It is geometrically demonstrated in the one-dimensional example of Fig. 1, meaning simply that the slope of the tangent to the energy curve at $k_z = k_0$ is larger than the slope of the chord $(1/\hbar)(\mathscr{E}_{k_{zb}} - \mathscr{E}_{k_{za}})/(k_{zb} - k_{za}) = \omega/q \equiv v_{ph}$.

In free space ($v_{ph} = \omega/q = c$) Eqs. (3) and (4) can never be simultaneously satisfied, and a situation where the electron-beam group velocity exceeds the speed of light c, (8), cannot take place. The only solution of (3, 4) in free space is the null solution $\omega = q = 0$. In order to balance the conservation Eqs. (3, 4) for nonvanishing frequencies, a perturbation must be introduced to the electron electromagnetic wave system which will effect either the electron wave or the electromagnetic wave, so that interaction between the electrons and the electromagnetic wave and possibly lasing can take place[1]. We henceforward discuss three techniques to introduce such a perturbation which also defines three kinds of free-electron lasers.

Cerenkov-Smith-Purcell Lasers

If the electromagnetic wave propagates in matter with index of refraction $n > 1$, then $v_{ph} = c/n$ is smaller than the speed of light c and there is no reason why the Cerenkov condition (8) cannot be satisfied and radiation gain becomes available. The satisfaction of the conservation Eqs. (3, 4) becomes possible in this case by perturbing the electromagnetic wave and increasing its momentum $q = n\omega/c$ ($n > 1$) so that the conservation of momentum condition can be satisfied.

[1] If the electron wave is being perturbed the electron is no longer a free electron and possibly the choice of name "free-electron lasers" may be somewhat disturbing. "Electron-beam lasers" may be a more accurate name to describe the devices presently discussed

Satisfaction of (8) is also possible if the electromagnetic wave propagates in a "periodic slow wave structure" [1], in which the eigenmodes of the electromagnetic wave have components which propagate at phase velocity much smaller than the speed of light.

If the periodic structure has periodicity in the z direction with period L, then its electromagnetic eigenmode waves have the Floquet-Bloch form

$$A(r,t)=\sum_{m=-\infty}^{\infty} A_m(x,y)\exp(i\beta_m z-i\omega t) \tag{9}$$

$$\beta_m\equiv\beta_0+m\frac{2\pi}{L}. \tag{10}$$

Apparently, the components of the wave (space harmonics) may have a phase velocity considerably lower than the speed of light c. For example, the first-order space harmonic ($m=1$) has the phase velocity $v_{ph_1}=\omega/\beta_1=\omega/(\beta_0+2\pi/L)<c$ and the inequality becomes stronger, the smaller is the period L.

We can understand that radiative transitions can take place in a periodic structure also by noticing that instead of the third Eq. (2) we can use (9) in (1). In free space, we know that the matrix element vanished because (3) would not be satisfied simultaneously with (4). However, in the periodic structure where we use (9), we can have a nonvanishing matrix element if we choose the period L so that (4) is satisfied with β_m instead of q, so that

$$k_i-k_f=\beta_m \tag{11}$$

instead of (4). We will call this phase matching through the m order space harmonic of the electromagnetic wave. Physically, it can be argued that we used the "crystal momentum" $m2\pi/L$ in order to balance the unbalanced momentum conservation Eq. (4). This process is illustrated in Figs. 1 and 2a.

Spontaneous emission of radiation in the visible frequency regime from an electron beam propagating in a periodic structure (optical grating) was first observed by Smith and Purcell [2]. Also the Traveling Wave (TW) tube amplifier is a device which is based on electron beam interaction with electromagnetic wave (in the microwave regime) in a periodic structure (helix, periodic waveguide) which effects the electromagnetic wave. In contrast to the Smith-Purcell effect the TW tubes operate usually as stimulated emission devices. They also operate in the collective electron interaction regime, while the Smith-Purcell radiation is basically a single electron interaction effect. These differences will be explained in greater detail in the following sections.

Bremsstrahlung Lasers

It is possible to construct a periodic structure that will effect the electrons in the electron beam instead of the electromagnetic wave as in the previous case. The periodic structure can be a magnetostatic or electrostatic field which varies periodically along the direction of the beam propagation.

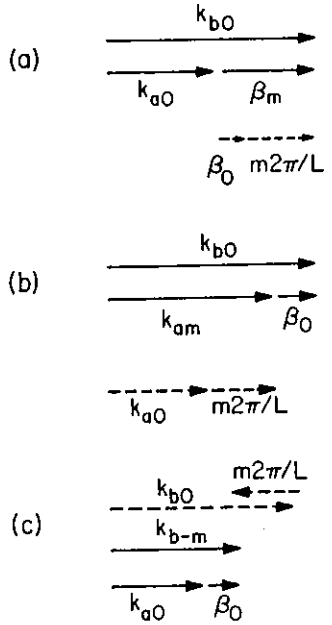

Fig. 2a—c. The three basic schemes of electron interaction with electro-magnetic wave in the longitudinal direction in a periodic structure: (a) Involving space harmonic (mth order) of the electromagnetic wave; (b) and (c) Involving space harmonics (m and $-m$ order) of the final and initial electron states waves, respectively

Just as in the previous case, the electron waves will have the Floquet-Bloch form. Consequently, radiative transitions can take place due to interaction via space harmonics of the initial or final electron state waves. These processes are described schematically in Fig. 2b, c. In addition to the process which involves phase matched interaction through the m order space harmonic of the electromagnetic wave (Fig. 2a), we may have a process which involves the m order space harmonic of the low energy electron state (Fig. 2b) or the $-m$ order space harmonic of the high energy electron state (Fig. 2c). The lattice momentum $|G|=m2\pi/L$ which is picked up this time by the electron waves, again helps to balance the momentum conservation Eq. (4) and make electron radiative transitions possible.

The Cerenkov-Smith-Purcell laser can be compared schematically with the bremsstrahlung laser by using Feynman diagrams, which describe the same three processes shown in Fig. 2 in terms of the free-space modes (or single harmonic waves) of electron waves and electromagnetic waves. Processes (b) and (c) of Fig. 3 correspond to the conventional Feynman diagrams for bremsstrahlung. In (b) an electron emits a photon and the momentum is conserved due to the elastic scattering of the electron in its final state, picking up momentum G

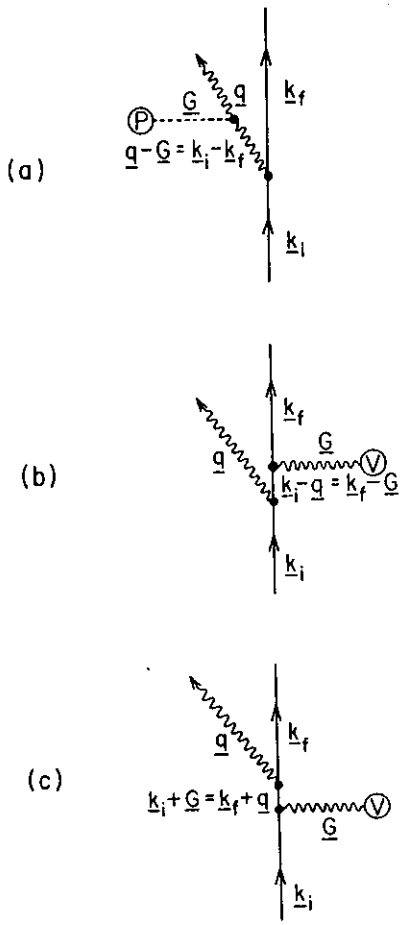

Fig. 3a—c. Feynman diagram representation of the three radiative emission processes of Fig. 2. (a) Momentum is conserved in the process by elastic scattering of a photon (Cerenkov, Smith-Purcell), (b) and (c) Momentum is conserved by elastic scattering of the electron in the final (b) or initial (c) state (bremsstrahlung)

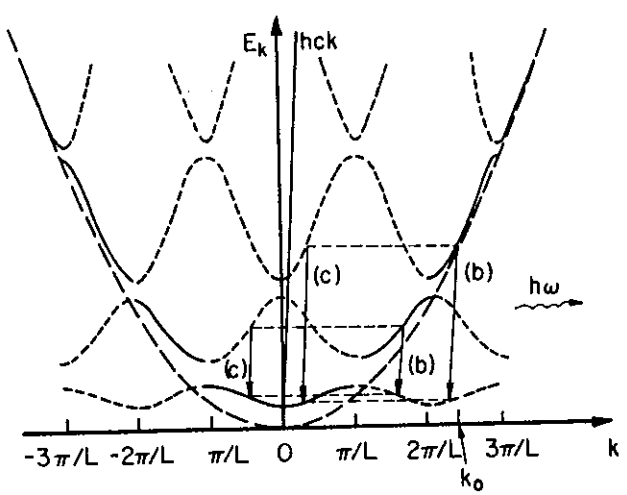

Fig. 4. The Brillouin band diagram of bremsstrahlung free-electron laser. Transitions (*b*) and (*c*) correspond to schemes (b) and (c) in Fig. 2

from the periodic potential. In (c) the electron is first scattered and then emits a photon[2]. Process (a) is a generalization of Feynman diagrams which represents schematically the interaction in the previously discussed Cerenkov-Smith-Purcell free electron laser. It corresponds to process (a) in Fig. 2 and describes the emission of a photon by the electron where in this case the photon is being elastically scattered from a periodic polarizable charge (P) and peaks up the missing crystal momentum G.

Notice that in both the Cerenkov-Smith-Purcell and the bremsstrahlung processes (Fig. 3a–c) the kinematics are the same. In all cases, a crystal momentum G is used to balance the momentum conservation Eq. (4). The difference is in the dynamics. The scattering process in schemes (b) and (c) of Fig. 3 is derived using the electron equation (Dirac equation), while the scattering process in scheme (a) is derived from Maxwell equations.

The laser action of a bremsstrahlung laser can be best understood from the Brillouin diagram of the electrons in the periodic structure (Fig. 4) which shows the quantum states between which the laser transitions take place. This diagram is the analog of Fig. 1 (which describes the Cerenkov-Smith-Purcell laser). According to this diagram the electrons injected into the periodic structure populate bands in the Brillouin diagram (analogously to the case of electrons in the periodic crystal lattice) and the laser electronic transitions correspond to interband radiative transitions.

The magnetic bremsstrahlung free-electron laser was demonstrated by a group in Stanford [3]. The device exhibited stimulated emission of $\lambda = 10.6\,\mu m$ radiation and operated with a high energy (24 MeV) linear accelerator electron beam. Recently also a free electron laser oscillator was reported by the same group, operating at $\lambda = 3\,\mu m$ wavelength [72].

The Stanford free-electron laser is basically a single-electron interaction device. However, we note that just as in the case of Cerenkov-Smith-Purcell lasers, *collective* interaction of an electron beam and an electromagnetic wave in a periodic *potential* structure is also possible. This is demonstrated in the microwave regime by the velocity jump amplifier [4] and the Ubitron [5].

Transverse Confining Force Free-Electron Laser

In the Cerenkov-Smith-Purcell and the bremsstrahlung free-electron lasers, conservation of energy and momentum (and consequently interaction) are made possible by a perturbation which modifies the momen-

[2] The two Feynman diagrams of bremsstrahlung represent the two terms of the second-order perturbation solution of *Dirac* equation in terms of the scattering potential and the scattering radiation potential

tum conservation Eq. (4). If a transverse confining force is applied to an electron beam, it is possible to get conservation of energy and momentum (and consequently interaction between the electrons and the electromagnetic wave) due to modification in the energy conservation Eq. (3).

If for the sake of simplicity we assume that the electrons are described by the Schrodinger equation (non-relativistic electrons), then in the presence of a transverse confining potential, the electron wave function $\psi(r)$ is described by

$$-\frac{\hbar^2}{2m}\left(\frac{\partial^2}{\partial z^2}+\nabla_\perp^2\right)\psi(r)+V(r_\perp)\psi(r)=E\psi(r), \tag{12}$$

where z is the electron beam propagation direction and the confining potential $V=V(r_\perp)$ is only a function of the transverse coordinates.

Consequently the electron wave function is separable to longitudinal and transverse parts

$$\psi(r)=\chi(r_\perp)\,e^{-ikz} \tag{13}$$

and from (12)

$$\left[-\frac{\hbar^2}{2m}\nabla_\perp^2+V(r)\right]\chi(r_\perp)=\left(E-\frac{\hbar^2k^2}{2m}\right)\chi(r_\perp). \tag{14}$$

Since the transverse potential is spatially confining the electrons we will have discrete eigenvalue solution to (14), hence

$$E=E_{mn}(k)=E_{mn}^{(0)}+\frac{\hbar^2k^2}{2m}. \tag{15}$$

The energy-momentum diagram will then look as in Fig. 5. It is apparent that radiative transitions conserving energy and momentum can take place, emitting a photon either in the forward or the backward direction. This kind of free-electron laser is more analogous to the conventional gas laser than the other ones. However, instead of distinct atomic energy levels the energetic levels are characterized by only two distinct quantum numbers. The laser can be thus regarded as being made of an "elongated atom" confined in the transverse direction and virtually infinite in the longitudinal direction. Of course, in this case the length of the atom is larger than the radiation wavelength. Hence, the conventional dipole approximation, used in the calculation of interaction between radiation and atoms, fails, and stronger interaction is expected.

The most familiar example of a transverse confining force free-electron laser is the cyclotron resonance maser [6]. In this case, the transverse confining force is provided by longitudinal magnetic fields, and the energy levels between which transitions take place (see Fig. 5) are the Landau levels [7].

Like in any laser, the condition for gain in the transverse force free-electron laser is population inversion. This

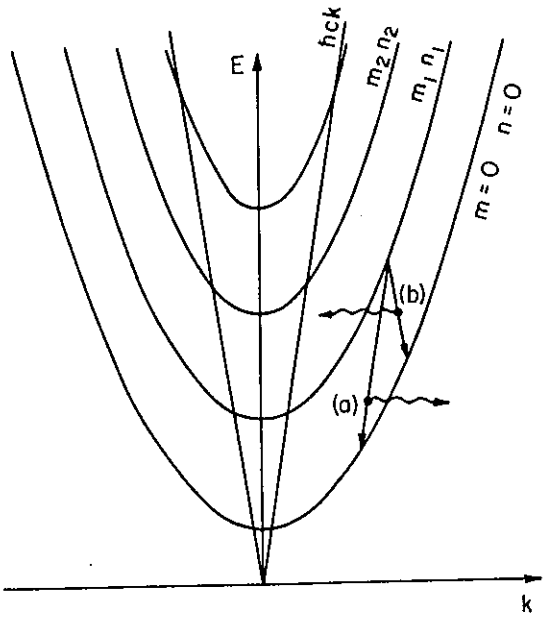

Fig. 5. Radiative transitions of free electrons in transversely confining potential. (*a*) forward emission process (*b*) backward emission

means that the electrons should be injected into a high energy state (e.g., m_1, n_1 in Fig. 5) so that they acquire transverse energy. If the longitudinal momentum spread of the electron beam is small, they will make narrow band transitions to a lower energy level (e.g., $m=0$ $n=0$), emitting radiation mostly on account of their transverse energy. Of course, it is possible to get also transitions between more separated levels and thus get emission of higher frequency radiation. This is called higher harmonic operation.

In the case of an harmonic oscillator transverse potential, which includes also the case of the non-relativistic cyclotron resonance maser, the spacing between the different energy curves is equal. Since the momentum of the emitted photon is usually small compared to the longitudinal momentum spread of the electron beam, the transitions (*a*) and (*b*) in Fig. 5 are almost vertical. Consequently absorptive transitions from level m_1, n_1 to level m_2, n_2 are as probable as emissive transitions from level m_1, n_1 to level $m=0$ $n=0$. In this case, of course, lasing is not possible. In the case of relativistic electrons, the Landau levels are not equispaced which makes operation of the electron cyclotron maser possible.

Another very interesting effect, which would provide radiation from an electron beam in the x-ray regime has been recently suggested. This effect [8, 9] "channeling radiation" operates on the same principle of emission from electrons in a transverse confining force and is analogous to the cyclotron resonance maser. The radiation in this case is emitted from electrons or positrons which channel through the crystal atomic

planes. The transverse confining force in this case is the crystaline field which keeps the electrons or the positrons confined in the channel. Of course, the classical Schrodinger equation (12) is not appropriate to be used in this case. However, relativistic quantum mechanical equations can be approximated into classical-like equations and the results are similar. The diagram of Fig. 5 thus describes the emission of x-ray radiation in the "channeling radiation" effect as well as the emission of microwave radiation from the cyclotron resonance maser.

1. Review of Experimental and Analytical Methods

The field of electron beam interaction with electromagnetic waves and particularly radiative emission from electron beams, is too wide to be covered by the present review and we will not attempt to list the numerous contributions to this field. We would rather try to present the different experimental and theoretical approaches taken in this field, putting special emphasis on those which are directly relevant to free-electron (or electron beam) lasers.

The two major research efforts in this field were pursued quite independently in the disciplines of physics and electrical engineering. Many fundamental effects involving radiative emission from electron beams were discovered and investigated by physicists in the past. Some of these effects are the Cerenkov radiation [10] (emission from electrons passing in or near a dialectric material), bremsstrahlung [11] (emission from decelerated electrons), Smith-Purcell radiation [2] (emission from electrons passing near an optical grating) and the cyclotron resonance maser [6] (emission from electrons in a uniform magnetic field). The possibility of stimulated emission by some of these effects was investigated by a number of investigators [12–14]. Some incoherent radiative devices were also constructed utilizing these effects [15, 16].

Important development of radiative electron beam devices evolved in the discipline of electrical engineering from the radio electron tubes technology. This started with the development of the klystron and the traveling wave tube amplifier in the nineteen forties [17]. It was followed by the development of a specialized analytical formalism to describe these devices [1] and the development of many other radiative electron tube devices like the magnetron, crossed field tube and others [18]. The analytical methods used in the description of these electron tube devices were often quite different from methods used in physics to describe different basic effects like the Cerenkov radiation bremsstrahlung, Smith-Purcell radiation and Compton scattering. Thus, little was done to understand the relation between the different, but fundamentally related effects and devices and to bridge the different analytical techniques used [19, 20, 14].

In the field of electron tubes the electron beams were usually produced by thermal emission cathodes and accelerated by anode voltages of the order of few KeV to tens of KeV. Operation range was usually in the microwave frequency regime up to millimeter wavelengths. The analysis of these tubes is usually done in terms of space charge waves (longitudinal plasma waves of the beam) [1]. This analysis fails in regimes where the electron beam density becomes too low, when the velocity spread is too large or when the radiation frequency is too high [21, 22]. In these cases the devices operate in the single-electron interaction regime and the collective effects (the plasma space charge waves) are negligible. The strength of the interaction is smaller in the single-electron regime. For this reason, and also because of some technological limitations, it was hard to operate such devices at wavelengths shorter than 1 mm [23].

The experiments involving the different physical effects were usually done in the single-electron interaction regime using high energy low density electron beams and high frequency radiation. The Smith-Purcell experiment [2] was demonstrated using a 300 KeV electron beam produced by a Van der Graaff accelerator. Radiation was measured in the visible light wavelength region. Cerenkov radiation experiments were usually done using very high energy electron beams (MeV to GeV) produced by linear accelerators [12].

The recent free-electron laser experiment which was carried out in Stanford University [3] has aroused considerable interest in this field. This experiment used a high energy (24 MeV) electron beam which was produced by a linear accelerator. It demonstrated amplification of 10.6 μm wavelength radiation using the mechanism of magnetic bremsstrahlung. This experiment demonstrated for the first time amplification of optical radiation by stimulated emission from accelerated electrons operating in the single-electron interaction regime. Recently this device was operated also as an oscillator [72].

The magnetic bremsstrahlung free electron laser was analyzed by a number of workers using different approaches. The principle of the device is related to that of the "Ubitron", in which microwave radiation is emitted from an undulated electron beam. Such devices were investigated and analyzed earlier by means of classical electron tube theory [5, 24]. Palmer [25] has presented a classical analysis of a structure essentially similar to the structure of Stanford's free electron laser. He investigated the operation of such a device both as a laser and as a linear accelerator (in which case the laser "operates inversely" and accelerates electrons by absorbing radiation). Madey [14] analyzed the magnetic

bremsstrahlung free-electron laser using a relativistic quantum mechanical calculation of Compton scattering. He approximated the periodic magnetostatic field by a plane wave of zero frequency which in the relativistic electron rest frame looks like an incoming real photon and is scattered by it according to the rules of Compton scattering. Sukhatme and Wolf [26] used a similar approach in investigating the problem of stimulated Compton scattering. The expression for gain derived by them differs from Madey's expression only by a small numerical factor. Hopf et al. [27] have recently published a rigorous classical analysis of this device by solving simultaneously to first order the coupled Boltzmann equation and Maxwell equations. They hence proved that the effect is essentially classical. Their expression for gain again differed from Madey's result only by a small factor.

Another very fruitful field of research, which is relevant to our discussion, has evolved recently with the development of very high intensity relativistic electron beam machines with cold field effect cathodes [28] and the investigation of their radiative emission. The high current density (and correspondingly high electron plasma density) enables one to obtain strong collective interaction and intense radiative emission in the microwave to submillimeter wavelength region by means of all of the interaction mechanisms discussed before.

Short pulses of high-power microwave radiation (10 MW) were produced from intense relativistic electron beams (40 KA, 500 KeV) generated by a cold field effect cathode electron beam accelerator [29, 30]. The radiation was generated by the interaction of the electron beam with the electromagnetic wave in a slow-wave structure (a periodically corrugated waveguide). These devices are therefore a "gigantic version" of the conventional traveling wave tube.

Another interesting experiment done with an intense relativistic electron beams is the demonstration of coherent Cerenkov radiation in the collective interaction regime [31]. In this experiment about 1 MW of microwave power was produced by the electron beam which passed through a hollow dielectric waveguide. Related experiments in the microwave regime were also suggested before [32] and are different from conventional Cerenkov radiation effect by involving collective rather than single-electron interaction, and allowing stimulated emission or amplified spontaneous emission (rather than spontaneous emission). The device may be right fully regarded as a gigantic traveling wave tube in which the dielectric waveguide is used as a slow wave structure instead of a helix or a periodic waveguide.

Experiments which involve microwave emission from an intense relativistic electron beam traversing a periodic magnetic field were also demonstrated [33, 34]. The recent experiment of Efthimion and Schlesinger [34] showed that the radiation wavelength dependence on periodicity is similar to that measured by Elias et al. [3], see (98). Thus this effect can be rightfully regarded as the "collective interaction analogue" of the Stanford free-electron laser experiment. While the Stanford experiment was presented and analyzed as stimulated Compton scattering of a zero-frequency pump by a single electron [14], its collective analog was described as stimulated Raman scattering of a zero frequency pump by the collective electron plasma wave of the beam [34]. However this device is not different in principle from the previously suggested Ubitron [5] except that it operates in the relativistic region and that an axial magnetic field exists along the interaction region in addition to the periodic field and thus cyclotron resonance effects take part in the interaction. A relativistic analysis of a similar structure, including the effect of the homogeneous axial magnetic field has been presented by Manheimer and Ott [35].

Extensive research and considerable amount of interest have evolved recently around the field of intense microwave emission by electron cyclotron masers. The early work [36, 37] used low energy (KeV to tens of KeV) electron beams produced by thermionic cathodes, and generated low levels of microwave power (1 Watt). Russian investigators [38, 39] have improved considerably the efficiency of these devices. Their versions of cyclotron resonance masers, called gyrotrons, produced microwave power of the order of tens of KW using low energy (tens of KV) electron beams produced by thermionic cathodes. They also obtained efficient operation at higher harmonic frequencies. Orders of magnitude increase in the output power of cyclotron resonance masers has been obtained with the introduction of the intense relativistic electron beam machines. Pulsed microwave power of the range of MW to GW was obtained in experiments where intense relativistic electron beams interacted with electromagnetic modes which propagated inside a wave guide in the presence of a uniform longitudinal magnetic field [33, 40–42].

In addition to cyclotron resonance radiation, also stimulated Raman scattering from the intense beam plasma wave was measured in some experiments. Submillimeter wavelength radiation was produced by scattering longer wavelength radiation which propagated opposite to the electron beam streaming direction [43, 44]. In a recent experiment generation of 1 MW power at 400 μm wavelength was reported [45]. Analysis of the stimulated collective scattering process was presented [46] and it was also shown that increased Raman scattering is obtained in the presence of an axial magnetic field due to cyclotron resonance effects [47]. Independent theoretical work [26, 48–51] was done

also in the single-electron regime where the analogous effect is stimulated Compton scattering and various schemes for Compton lasers (or parametric amplifiers) in the far infrared to x-ray regions were considered. The single electron effect is, of course, much weaker than the collective effect and should give discouragingly low stimulated emission gain at short wavelength [48, 50]. However similarly to the Raman scattering stimulated Compton scattering gain can also be increased by a cyclotron resonance effect produced by a longitudinal uniform magnetic field [51].

The coherent x-ray (on γ-ray) radiative emission of an accelerated electron in the crystal lattice is an intriguing possibility which was investigated by a number of investigators. Even though the experimental and theoretical techniques used in this field of research are quite different from those used in free-electron laser investigations, the principles of the different possible effects are similar and deserve discussion under the same framework.

In addition to the channeling radiation phenomenon [8, 9]; which is based on the transverse force which is exerted by the crystaline planes on channeling electrons or positrons, one would expect electron-electromagnetic wave interactions which are made possible by means of the natural crystal lattice periodicity.

Just as in artifical periodic structures, the electron and the electromagnetic waves which propagate in the periodic crystal are composed of Floquet-Bloch wave space harmonics and thus can interact via the bremsstrahlung or the Cerenkov mechanisms discussed above (Figs. 1–4). The bremsstrahlung process called "coherent bremsstrahlung" was investigated by a number of workers both theoretically [52–54] and experimentally [55–57]. In the experiment of Walker et al. [57], 28 MeV electron or positron beams produced in a linear accelerator, penetrated a 5 μm thick single crystal of silicon. A coherent peak near radiation energy of 0.5 MeV was observed. The effect measured was indeed detectable but very weak. The coherent bremsstrahlung effect is schematically described by diagrams (a) and (b) of Fig. 3. One would expect also "coherent Cerenkov" interaction via scheme (c) (in analogy to the Smith-Purcell effect). The analysis of electron radiative emission in the crystal via this mechanism was hardly treated in the literatur [21]. Some further discussion of this process is presented in Sec. 6.

Finally, it is proper to mention here the research on semiconductor radiative devices in which the interaction takes place with drifting carriers in the semiconductor, which drift through artifical periodic structures or superlattices. This field of research is quite detached from the research on free-electron lasers. However, the principles are similar, and gain may be obtained in either a Smith-Purcell-Cerenkov free-electron laser structure (schematically described by Fig. 1 and diagram c of Fig. 2) [69] or in a bremsstrahlung laser structure (schemes *b*, *c* in Figs. 2, 4) [58].

2. Coupled-Modes Analysis of Traveling Wave Interaction in Periodic Electromagnetic Structures

In the following sections we focus our attention on the interaction of electron beams with electromagnetic waves which propagate in periodic structures or other slow-wave structures (Smith-Purcell-Cerenkov radiation).

We analyze the interaction between the electromagnetic wave and the electrons in a periodic structure using a one-dimensional model and a coupled mode technique [21, 69]. It is assumed that the electromagnetic mode which travels in the structure is of the form (9), and that an electron beam is traversing along the structure (z direction) and is affected by the space harmonics of the electromagnetic wave. At present we assume that the periodic structure of infinite length affects only the electromagnetic wave and not the electrons. The simplified unified model expressions derived in this section will then be used in the following sections to delineate different operational regimes such as collective, single-electron, quantum-mechanical and classical regimes.

Concentrating on the z field component of one of the space harmonics we find that the electron beam plasma will be modulated longitudinally by an "external field" $E_{cz}(z,t)=E_{cz}(\beta,\omega)\exp(\mathrm{i}\beta z-\mathrm{i}\omega t)$, where $\beta\simeq\beta_m$ (β is the propagation constant of the coupled excitation, β_m is the propagation constant of the electromagnetic space harmonic m in the absence of interaction, given by (10)). This "external field" corresponds to the electric field of one of the space harmonics of the periodic structure which is close to synchronium with the electron beam. This will produce space charge current density $J_z(z,t)=J_z(\beta,\omega)\exp(\mathrm{i}\beta z-\mathrm{i}\omega t)$

$$J_z=-\mathrm{i}\omega\chi_p(\beta,\omega)E_z\,, \tag{16}$$

where $\chi_p(\beta,\omega)$ is the plasma susceptibility, E_z is the local field which is experienced by the plasma: $E_z=E_{cz}+E_{pz}$, where E_{pz} is the plasma space charge field and is found using the Poisson and continuity equations

$$\mathrm{i}\beta E_p=\varrho/\varepsilon=-\mathrm{i}\beta\chi_p(\beta,\omega)E_z/\varepsilon\,. \tag{17}$$

Hence we obtain

$$E_z=\varepsilon_p(\beta,\omega)E_{cz} \tag{18}$$

$$J_z=\frac{\mathrm{i}\omega\chi_p(\beta,\omega)}{\varepsilon_p(\beta,\omega)}E_{cz}\,, \tag{19}$$

where

$$\varepsilon_p(\beta,\omega)\equiv 1+\chi_p(\beta,\omega)/\varepsilon\,, \tag{20}$$

where ε is the dielectric constant of the medium excluding the electron beam contribution.
Equation (19) is a general linear plasma response expression which also includes the effect of plasma oscillation: In the particular case when the external field is $E_{cz}=0$, a finite current J_z may exist according to (19) only if the denominator vanishes

$$\varepsilon_p(\beta,\omega)\equiv 1+\chi_p(\beta,\omega)/\varepsilon=0. \tag{21}$$

This is the plasma dispersion relation, and its solutions are the longitudinal plasma space charge waves.
To complete the coupled mode analysis we need, in addition to (19), an expression for the field E_{cz} which would be induced in the slow wave structure by the current J_z. This dependence can be deduced from Maxwell equations, and is approximately given by Pierce's equation [1]

$$E_{cz}=-i\frac{\beta^2\beta_m K_m S}{\beta_m^2-\beta^2}J_z, \tag{22}$$

where S is the interaction cross section area, β_m of (10) is the wave number of space harmonic m (through which the interaction takes place) when there is no coupling, and K_m is the interaction impedance [1] of the space harmonic m. The interaction impedance

$$K_m\equiv\frac{|E_{zm}|^2}{2\beta_m P} \tag{23}$$

is characteristic of the electromagnetic mode. P is the total power in the mode.
The dispersion equation of the coupled excitation is obtained by imposing self consistency on (19) and (22). This yields

$$\frac{K_m S\beta_m\beta^2\omega}{\beta^2-\beta_m^2}\frac{\chi_p(\beta,\omega)}{1+\chi_p(\beta,\omega)/\varepsilon}=1. \tag{24}$$

In the limit of no coupling ($K_m=0$) the solutions of (24) are $\beta=\pm\beta_m$ and the roots of (21). These are the eigenmodes of the uncoupled systems: the circuit electromagnetic waves and the plasma waves, respectively. In the limit of small coupling the solutions of (24) are close to the uncoupled modes. We can then solve for the "electromagnetic-like" mode, using first-order expansion of β: $\beta=\beta_m+\Delta\beta$. Assuming that (21) has no roots near $\beta=\beta_m$, we get

$$\Delta\beta=\frac{1}{2}K_m S\beta_m^2\omega\frac{\chi_p(\beta_m,\omega)}{1+\chi_p(\beta_m,\omega)/\varepsilon}. \tag{25}$$

In particular

$$\mathrm{Im}\{\beta\}=\mathrm{Im}\{\Delta\beta\}=\frac{1}{2}K_m S\beta_m^2\omega\frac{\mathrm{Im}\{\chi_p(\beta_m,\omega)\}}{|1+\chi_p(\beta_m,\omega)/\varepsilon|}. \tag{26}$$

3. Single Electron Interaction

When (21) does not have a root near $\beta=\beta_m$, the electromagnetic wave does not couple strongly to the collective excitation of the electron beam plasma. The interaction then is basically an individual free-electron interaction. The solution of (24) is then given (to first order) by (25), (26) and the exponential gain of the coupled excitation is calculated by $\alpha=-2\,\mathrm{Im}\{\beta\}$.
In order to get some quantitative estimate of the gain, one must first derive the longitudinal plasma suspectibility $\chi_p(\beta,\omega)$. In a quantum mechanical model the susceptibility of a free-electron plasma is given by the Lindhard function [59]. This function is derived in the nonrelativistic limit by solving for the plasma response to the first-order perturbation Hamiltonian (1) [21, 69].

$$\chi_p(\beta,\omega)=\frac{1}{(2\pi)^3}\frac{e^2}{\beta^2}\int\frac{f_0(k+\beta)-f_0(k)}{\hbar\omega-(\mathscr{E}_{k+\beta}-\mathscr{E}_k)+i\eta}d^3k \tag{27}$$

where $\mathscr{E}_k=\hbar^2k^2/(2m)$ is the free-electron energy, $f_0(k)$ is the occupation number of electronic state k, $\beta=\beta\hat{e}_z$, and η is an infinitesimal positive parameter (when collisions are considered, $\eta=\hbar/\tau$ is finite, where τ is the collision relaxation time).
Setting in (27) $\beta=\beta_m=\beta_m\hat{e}_z$ and $\eta\to 0^+$, we get

$$\mathrm{Re}\{\chi_p(\beta_m,\omega)\}=\frac{1}{(2\pi)^3}\frac{e^2}{\beta_m^2}\cdot\mathscr{P}\int\frac{f_0(k+\beta_m)-f_0(k)}{\hbar\omega-(\mathscr{E}_{k+\beta_m}-\mathscr{E}_k)}d^3k \tag{28}$$

$$\mathrm{Im}\{\chi_p(\beta_m,\omega)\}=-\frac{\pi}{(2\pi)^3}\frac{e^2}{\beta_m^2}\int[f_0(k+\beta_m)-f_0(k)]\cdot\delta[\hbar\omega-(\mathscr{E}_{k+\beta_m}-\mathscr{E}_k)]d^3k. \tag{29}$$

Expression (29) vividly demonstrates the conclusions which were derived from general considerations in the introduction. Only transitions which conserve both energy and momentum

$$\mathscr{E}_{k_b}-\mathscr{E}_{k_a}=\hbar\omega \tag{30}$$

$$k_b-k_a=\beta_m \tag{31}$$

contribute to the integral in (29). Since the gain of the electromagnetic wave $\alpha=-2\,\mathrm{Im}\{\beta\}$ is proportional to $\mathrm{Im}\{\chi_p\}$, (26), we find that only transitions between states which fulfill (30), (31) contribute to electromagnetic wave amplification (stimulated emission) or attenuation (stimulated absorption). There will be net attenuation of the electromagnetic wave if the population of the lower states k_a is higher than that of the higher states $k_b=k_a+\beta_m$ (as is the case in thermal equilibrium distribution). In the opposite case we have a situation of population inversion and net gain may be attained.

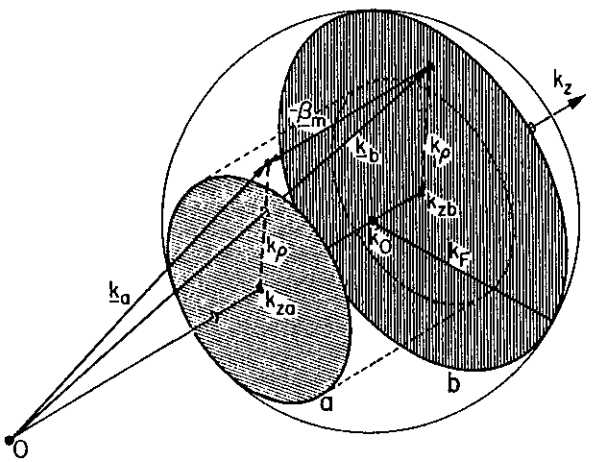

Fig. 6. Radiative transitions from an electron beam with a shifted Fermi sphere distribution

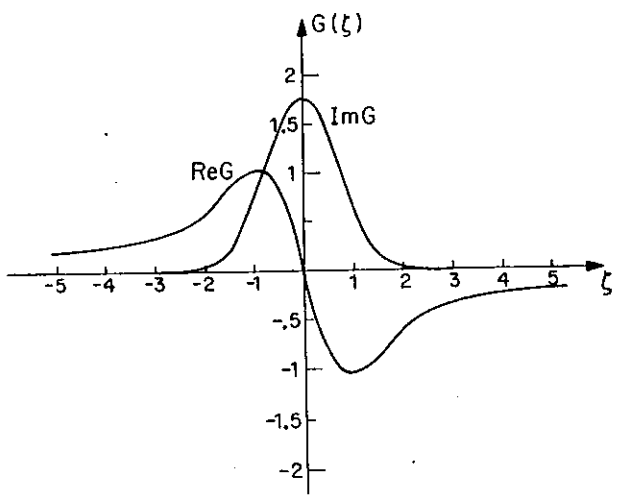

Fig. 7. The plasma dispersion function $G(\zeta)$ for a Maxwellian distribution and real argument ζ

Figure 6 is a three-dimensional illustration of the permitted electronic transitions, satisfying (30, 31), in the case where the electron distribution is a shifted Fermi sphere centered at $k=k_0\hat{e}_z$ and of radius k_F. Noting that $\beta_m=\beta_m\hat{e}_z$ we find that the geometrical location of all the pairs of electronic states which are connected by (30), (31) are the two planes

$$k_z=k_{za}\equiv\frac{m}{\hbar}\frac{\omega}{\beta_m}-\frac{\beta_m}{2} \tag{32}$$

$$k_z=k_{zb}\equiv\frac{m}{\hbar}\frac{\omega}{\beta_m}+\frac{\beta_m}{2}=k_{za}+\beta_m. \tag{33}$$

Hence in this example the geometrical meaning of the population inversion condition is that the area of circle b would be larger than that of circle a. The gain according to (26) and (29) would be proportional to the difference between the areas of the two circles.

We find that for nonrelativistic electrons $\mathscr{E}_{k+\beta_m}-\mathscr{E}_k=(\hbar^2\beta_m/m)(k_z+\beta_m/2)$ is independent of the transverse components k_x, k_y. Therefore it is possible to integrate (28), (29) over these variables. We also define the normalized one dimensional distribution function $g(x)$

$$g\left(\frac{k_z-k_0}{k_{th}}\right)\equiv\frac{1}{(2\pi)^3}\frac{k_{th}}{n_0}\int f_0(k)dk_xdk_y, \tag{34}$$

where

$$n_0\equiv\frac{1}{(2\pi)^3}\int f_0(\boldsymbol{k})d^3k \tag{35}$$

$$k_0\equiv\frac{1}{(2\pi)^3}\frac{1}{n_0}\int k_z f_0(\boldsymbol{k})d^3k \tag{36}$$

$$k_{th}^2/2\equiv mk_BT/\hbar^2\equiv\frac{1}{(2\pi)^3}\frac{1}{n_0}\int(k_z-k_0)^2f_0(k)d^3k \tag{37}$$

and $\omega_p\equiv[n_0e^2/(\varepsilon m)]^{1/2}$ is the plasma frequency. The plasma dispersion function

$$G(\zeta)\equiv\int_{-\infty}^{\infty}\frac{g(x)}{x-\zeta}dx\qquad(\mathrm{Im}\,\zeta>0) \tag{38}$$

which in the limit $\mathrm{Im}\,\zeta\to0^+$ is

$$\mathrm{Re}\{G(\zeta)\}=\mathscr{P}\int_{-\infty}^{\infty}\frac{g(x)}{x-\zeta}dx \tag{39}$$

$$\mathrm{Im}\{G(\zeta)\}=\pi g(\zeta). \tag{40}$$

Consequently, (27) to (29) can be reduced to the simpler form

$$\chi_p(\beta_m,\omega)=-\frac{\varepsilon}{2}\frac{k_A^3}{\beta_m^3}[G(\zeta_b)-G(\zeta_a)] \tag{41}$$

and in particular

$$\mathrm{Im}\{\chi_p(\beta_m,\omega)\}=-\frac{\varepsilon}{2}\frac{k_A^3}{\beta_m^3}[\mathrm{Im}\{G(\zeta_b)\}-\mathrm{Im}\{G(\zeta_a)\}]$$
$$=-\frac{\pi}{2}\varepsilon\frac{k_A^3}{\beta_m^3}[g(\zeta_b)-g(\zeta_a)], \tag{42}$$

where

$$\zeta_a\equiv\frac{k_{za}-k_0}{k_{th}} \tag{43}$$

$$\zeta_b\equiv\frac{k_{zb}-k_0}{k_{th}} \tag{44}$$

$$k_A^3\equiv\frac{2\omega_p^2m^2}{\hbar^2k_{th}}. \tag{45}$$

In the case of a shifted Gaussian distribution function the normalized distribution function is $g(x)=(1/\sqrt{\pi})\exp(-x^2)$. The functions

$$\mathrm{Re}\{G(\zeta)\}=\frac{1}{\sqrt{\pi}}\mathscr{P}\int_{-\infty}^{\infty}\frac{e^{-x^2}}{x-\zeta}dx \tag{46}$$

$$\mathrm{Im}\{G(\zeta)\}=\sqrt{\pi}\,e^{-\zeta^2} \tag{47}$$

are plotted in Fig. 7, and tabulated in [60]. With these curves and (26), (41), (42) it is possible to calculate the electromagnetic gain $\alpha = -2\,\mathrm{Im}\{\beta\}$ for any specific case. Notice that from (26), (42) it follows that $\alpha = -2\,\mathrm{Im}\{\beta\}$ is positive (gain) only if

$$g(\zeta_b) > g(\zeta_a) \tag{48}$$

which is the gain condition (7) in terms of the normalized distribution function $g(\zeta)$.

In the case of a shifted Fermi sphere distribution (Fig. 6)

$$f_0(k) = \begin{cases} 2 & |k - k_0| \leqq k_F \\ 0 & |k - k_0| > k_F \end{cases} \tag{49}$$

we normalize the distribution function with k_F instead of k_{th}. Instead of (34) to (47) we have

$$g_F\left(\frac{k_z - k_0}{k_F}\right) \equiv \frac{1}{(2\pi)^3}\frac{k_F}{n_0}\int f_0(k)\,dk_x\,dk_y \tag{50}$$

$$G_F(\xi) \equiv \int_{-\infty}^{\infty} \frac{g_F(x)}{x - \xi}\,dx \quad (\mathrm{Im}\,\xi > 0) \tag{51}$$

$$\mathrm{Re}\{G_F(\xi)\} = \mathscr{P}\int_{-\infty}^{\infty} \frac{g_F(x)}{x-\xi}\,dx = -\tfrac{3}{2}\left[\xi + \tfrac{1}{2}(\xi^2 - 1)\ln\left|\frac{1-\xi}{1+\xi}\right|\right] \tag{52}$$

$$\mathrm{Im}\{G_F(\xi)\} = \pi g_F(\xi) = \begin{cases} \frac{3\pi}{4}(1-\xi^2) & |\xi| \leqq 1 \\ 0 & |\xi| > 1 \end{cases} \tag{53}$$

$$\chi_p(\beta_m, \omega) = -\frac{\varepsilon}{2}\frac{k_G^3}{\beta_m^3}[G_F(\xi_b) - G_F(\xi_a)] \tag{54}$$

$$\xi_b \equiv \frac{k_{zb} - k_0}{k_F} \tag{55}$$

$$\xi_a \equiv \frac{k_{za} - k_0}{k_F} \tag{56}$$

$$k_G^3 \equiv \frac{2\omega_p^2 m^2}{\hbar^2 k_F}. \tag{57}$$

The functions $\mathrm{Re}\{G_F(\xi)\}$ and $\mathrm{Im}\{G_F(\xi)\}$ are plotted in Fig. 8.

4. The Classical Limit

When $\beta_m \ll k_{za}$ we obtain from (32) and (33)

$$k_{za} \simeq k_{zb} \simeq \frac{m}{\hbar}\frac{\omega}{\beta_m}. \tag{58}$$

This condition can then be written as

$$\beta_m^2 \ll \frac{m}{\hbar}\omega \tag{59}$$

which is the classical limit condition.

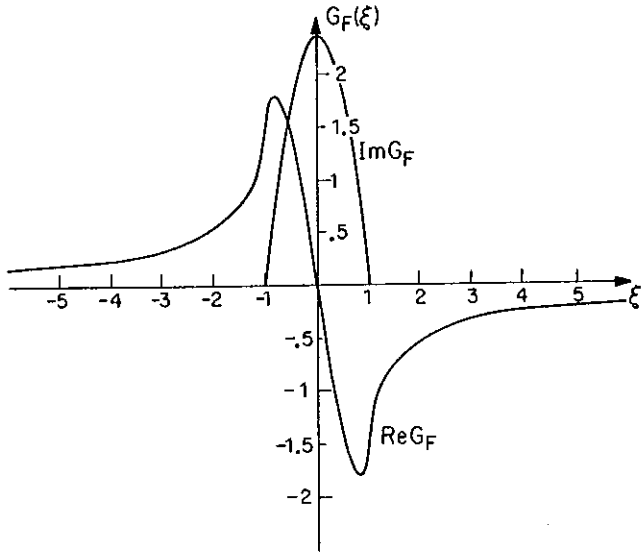

Fig. 8. The plasma dispersion function $G_F(\xi)$ for Fermi electron gas ($T = 0$)

In this limit we can replace the differences between the functions in (41) and (42) by differentials. The expressions for the plasma susceptibility (41, 42, 54) become

$$\chi_p(\beta_m, \omega) = -\frac{\varepsilon}{2}\frac{k_D^2}{\beta_m^2}G'(\zeta_m) \tag{60}$$

and particularly

$$\mathrm{Im}\{\chi_p(\beta_m, \omega)\} = -\frac{\varepsilon}{2}\frac{k_D^2}{\beta_m^2}\mathrm{Im}\{G'(\zeta_m)\} = -\frac{\pi}{2}\varepsilon\frac{k_D^2}{\beta_m^2}g'(\zeta_m) \tag{61}$$

for the nondegenerate plasma; and

$$\chi_p(\beta_m, \omega) = -\frac{\varepsilon}{2}\frac{k_{FT}^2}{\beta_m^2}G_F'(\xi_m) \tag{62}$$

$$\mathrm{Im}\{\chi_p(\beta_m, \omega)\} = -\frac{\varepsilon}{2}\frac{k_{FT}^2}{\beta_m^2}\mathrm{Im}\{G_F'(\xi_m)\} = -\frac{\pi}{2}\varepsilon\frac{k_{FT}^2}{\beta_m^2}g_F'(\xi_m) \tag{63}$$

for the degenerate (shifted Fermi sphere) distribution, where k_D is the Debye wave number

$$k_D^2 \equiv 2\frac{\omega_p^2}{v_{th}^2} \equiv \frac{k_A^3}{k_{th}} \tag{64}$$

$$\zeta_m \equiv \frac{\omega/\beta_m - v_0}{v_{th}} \tag{65}$$

$$v_{th} = \frac{\hbar}{m}k_{th} \tag{66}$$

$$v_0 = \frac{\hbar}{m}k_0 \tag{67}$$

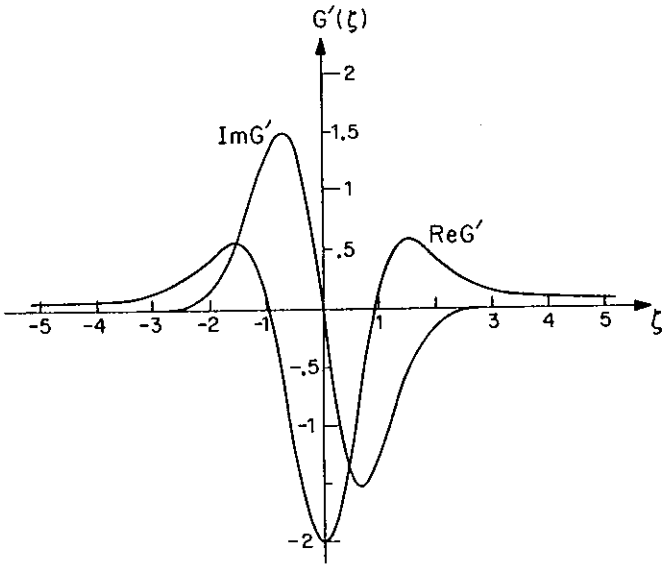

Fig. 9. The derivative of the plasma dispersion function $G'(\zeta)$ for Maxwellian distribution and real argument ζ

and k_{FT} is the Fermi-Thompson wave number

$$k_{FT}^2 \equiv 2\frac{\omega_p^2}{v_F^2} \equiv \frac{k_G^3}{k_F} \tag{68}$$

$$\zeta_m \equiv \frac{\omega/\beta_m - v_0}{v_F} \tag{69}$$

$$v_F \equiv \frac{\hbar}{m} k_F . \tag{70}$$

The functions $\mathrm{Re}\{G'(\zeta)\}$, $\mathrm{Im}\{G'(\zeta)\}$ are plotted in Fig. 9 and are tabulated in [60].

These expressions can be used in conjunction with (26) to compute the gain $\alpha = -2\mathrm{Im}\{\beta\}$. The population inversion condition (48) is reduced to

$$g'(\zeta_m) > 0 \tag{71}$$

which according to (26, 61) results in positive gain.

These results can be related to the "Landau damping" effect [61]. Landau solved the problem in the case of plasma in thermal equilibrium, where $g'(\zeta_m) < 0$ so that damping occurs. Our problem differs from Landau's problem in two aspects: (a) We allow for a drifting plasma so we can have $g'(\zeta_m) > 0$. (b) The presence of a periodic slow wave structure (external circuit) which can support rotational electromagnetic wave.

Instead of obtaining the classical expression for the susceptibility (60) by using the quantum mechanical expression (41) in the limit (59), one may derive it directly from the Boltzman equation which gives the same result [62]. By using the relativistic Boltzman equation, a relativistic modification to (60) results in

$$\chi_p = -\frac{\varepsilon}{2\gamma_0^3}\frac{k_D^2}{\beta_m^2} G'(\zeta_m), \tag{72}$$

where k_D and ζ_m are still defined by (64) and (65), respectively, but v_{th} is defined by

$$v_{th} \equiv \frac{\hbar}{m\gamma_0^3} k_{th} \tag{73}$$

instead of (66).

$$\gamma_0 \equiv [1-(v_0/c)^2]^{-1/2} . \tag{74}$$

Consequently in the relativistic regime the imaginary part of the susceptibility is given by

$$I_m\chi_p = -\frac{\varepsilon}{2\gamma_0^3}\frac{k_D^2}{\beta_m^2}\mathrm{Im}\{G'(\zeta_m)\} = -\frac{\pi}{2}\frac{\varepsilon}{\gamma_0^3}\frac{k_D^2}{\beta_m^2} g'(\zeta_m). \tag{75}$$

A necessary condition for the reduction to the classical limit of (60–63) is that the second order Taylor expansion of $g(\zeta_b) - g(\zeta_a)$ in terms of β_m will be negligible relative to the first-order term:

$$\beta_m \ll \left|\frac{2g'(\zeta_m)}{g''(\zeta_m)}\right| k_{th} . \tag{76}$$

This means that the variation in the electron distribution between states $k_{za} < k_z < k_{zb}$ should be gradual enough and not abrupt. In vacuum electron tube diodes the electron distribution falls abruptly to zero on the low velocity side of the distribution [63]. This velocity distribution edge corresponds to the electrons which leave the cathode vicinity with zero (thermal) kinetic energy. In this case, if the electromagnetic wave phase velocity $v_{ph_m} = \omega/\beta_m$ is synchronous with the slow edge of the electron distribution, and β_m is large enough, quantum effects may not be negligible and the first-order electromagnetic gain will still be proportional to a population difference $g(\zeta_b) - g(\zeta_a)$ – (26, 42)–rather than to the derivative of the distribution function $g'(\zeta_m)$, (26, 61).

In the case when $|\zeta| \gg 1$ we can substitute (38) (for any finite distribution function $g(x)$) by its asymptotic approximation

$$G(\zeta) \simeq -\frac{1}{\zeta} \tag{77}$$

When substituted in (60) this results in

$$\chi_p = -\varepsilon\frac{\omega_p^2}{(\omega - \beta v_0)^2} \tag{78}$$

which when substituted in (24) produces the conventional traveling wave amplifier dispersion equation [1]

$$-\frac{K_m S\beta_m\beta^2\omega\omega_p^2/v_0}{(\beta^2-\beta_m^2)\left[\left(\beta-\frac{\omega}{v_0}\right)^2 - \left(\frac{\omega_p}{v_0}\right)^2\right]} = 1 . \tag{79}$$

Notice that this equation is applicable *only* if

$$|\zeta| = \frac{|\omega/\beta - v_0|}{v_{th}} \gg 1, \tag{80}$$

which means that the phase velocity of the wave ω/β should be sufficiently out of synchronism with the electron beam velocity v_0, compared to its velocity spread v_{th}, so that the electron beam would look monoenergetic to the wave. In the limit of monoenergetic beam, indeed the electron beam plasma can be described by the macroscopic (moment) equations from which (79) was originally derived [1].

5. Collective Interaction

The formulation presented above is general and describes self-consistently the interaction of an assembly of electrons and an electromagnetic "circuit" wave. We can use it to delineate two extreme regimes: (a) Where the collective nature of the electrons (plasma waves) is important and (b) The single electron regime. Regime (a) obtains when the phase velocity of the "cold circuit" ω/β_m nearly equal to that of the plasma wave at the absence of the circuit i.e.,

$$\varepsilon_p(\beta_m, \omega) \equiv 1 + \chi_p(\beta_m, \omega)/\varepsilon \cong 0. \tag{81}$$

It follows from (19) that under these conditions the propagating disturbance is accompanied by strong ac excitation in the electron plasma so that we refer to it as the collective regime. The microwave traveling wave tube, as an example, operates in this regime.

The second regime is one where condition (81) is far from being satisfied. The interaction of the electromagnetic wave and the electron beam does not involve substantial excitation of the electronic plasma wave, and consequently, we refer to this regime as that of the single electron interaction. The Smith-Purcell or Cerenkov radiators fall in this category.

Notice that the gain (or population inversion) condition—(8 or 48 or 71)—is applicable in both the collective and single-electron regimes. In both cases we may get either gain or attenuation depending on whether the gain condition is satisfied or not. However, as (26) indicates, higher gain or attenuation are usually expected when the condition, (81), of plasmon-photon phase matching (collective interaction) can be approached.

When (81) is satisfied (collective interaction), the first-order solution (25) cannot be used. Instead, we may expand both denominators of (24) to first order near β_m and obtain a second-order equation for $\Delta\beta$ [21]. Sometimes even the second-order approximation is not valid (as can be the case in the traveling wave amplifier) and (24) must be solved accurately.

To get collective interaction in the nondegenerate plasma quantum mechanical regime, one has to satisfy (81) with the susceptibility χ_p given by (41). The real and imaginary parts of the function $G(\zeta)$ are illustrated in Fig. 7 for the case of shifted Gaussian distribution. By inspection we find that we cannot satisfy (81) unless

$$\beta_m \ll k_A. \tag{82}$$

The real part of (81) $1 - 0.5(k_A^3/\beta_m^3)\,\mathrm{Re}\,\{G(\zeta_b) - G(\zeta_a)\} = 0$ may be satisfied even with a weak inequality in (82). However for the imaginary part to diminish $\mathrm{Im}\,\{G(\zeta_b) - G(\zeta_a)\} \simeq 0$ one must satisfy the strong inequality (82) so that $|\zeta_a|, |\zeta_b| \gg 1$. Exact vanishing of $\mathrm{Im}\,\{G(\zeta_b) - G(\zeta_a)\}$ is never possible as long as the tail of the electron distribution does not vanish (which is the reason for the Landau damping effect). However, the larger $|\zeta_a|$, $|\zeta_b|$ are, the closer $\mathrm{Im}\,\{G(\zeta_b) - G(\zeta_a)\}$ approaches zero.

Similarly to the nondegenerate case, in the degenerate quantum case—(52 to 54) and Fig. 8—the condition for the satisfaction of (81) (collective interaction) is

$$\beta_m \ll k_G. \tag{83}$$

In the classical limit (60, 61) and Fig. 9—we must require

$$\beta_m \ll k_D \tag{84}$$

in order to satisfy (81) (collective interaction). Similarly in the classical degenerate limit—(62, 63, 81)—the condition for collective interaction is

$$\beta_m \ll k_{FT}. \tag{85}$$

An additional condition for obtaining collective interaction is

$$2\pi/\beta_m \gg n_0^{-1/3}, \tag{86}$$

which means that the longitudinal bunching period of the plasma should be considerably larger than the average distance between individual electrons, so that a continuous charge hydrodynamical model can be used for the plasma. A different interpretation of (84) and (86) is presented in the appendix. It is shown that (84) results from requiring that the collective longitudinal plasma bunching energy will exceed the individual thermal (escape) energy of the electrons, and (86) results from requiring that the collective energy exceeds the Coulomb repulsion energy between individual electrons.

Under conditions where collective interaction cannot take place, a theory which is based on plasma charge waves analysis [1] cannot be used. However our first-order single electron interaction analysis (Secs. 2, 3) still holds. We just need to avoid using Poisson equation (17) claiming that the electron plasma is dilute enough so that the local field $E_z(\beta, \omega)$ is identical to the external

field $E_c(\beta,\omega)$ and $\varepsilon_p(\beta,\omega)\simeq 1$, (18). So that our first-order single-electron interaction analysis (Sec. 3) can be used whenever conditions (85) (86) are not satisfied.

In the classical monoenergetic beam limit where (79) applies and we assume that collective interaction takes place, (81), we find from (81, 79) that

$$\frac{\omega}{\beta_m}\simeq v_0\pm\frac{\omega_p}{\beta_m}. \tag{87}$$

Since inequality (84) is necessarily satisfied when collective interaction takes place, we find from (64), (84), (87) that inequality (80) is automatically satisfied. This proves that in the classical regime (79) is usually applicable for traveling wave amplifiers operating at their normal (collective) operation condition, since then condition (80) is automatically satisfied.

The collective interaction of an electron beam with an electromagnetic wave may offer higher gain than the single-electron interaction mode. It is therefore a question of practical interest to find what is the theoretical upper frequency limit for operating traveling wave amplifiers in the collective mode [22]. This limit is usually defined by (84) and (86). However, in evaluating the Debye wave number k_D, (64), one has to recall that the velocity distribution spread v_{th} which appears in (64) is the longitudinal velocity spread of the electron beam, which in accelerated beams is usually very different from the transverse velocity spread [21, 63]. Assuming that the longitudinal velocity spread originates only from the initial thermal spread; then

$$v_{th}=\tfrac{1}{2}\frac{(v_{th})_i^2}{\gamma_0^3 v_0}, \tag{88}$$

where v_0 is the average velocity of the beam after acceleration and $(v_{th})_i$ is the initial thermal velocity before acceleration.

We find that the longitudinal velocity spread v_{th} of the accelerated beam can be many orders of magnitude smaller than the initial thermal velocity $(v_{th})_i$. The initial thermal velocity in a vacuum electron tube diode is about $(v_{th})_i=2.1\times10^7$ cm/s (corresponding to cathode temperature $T_i=1500$ K). Using (88) we find that the longitudinal velocity spread after acceleration to $v_0=4.5\times10^9$ cm/s (6 KeV energy) is only $v_{th}=5\times10^4$ cm/s.

Current densities of the order of 1 KA/cm^2 are available in traveling wave tubes [22] which at this velocity ($v_0=4.5\times10^9$ cm/s) translates into $n_0=1.4\times10^{12}\,cm^{-3}$ *and* $\omega_p=6.6\times10^{10}$ rad/s. With the use of (64) we obtain that $k_D=1.9\times10^6\,\mathrm{cm}^{-1}$ and also that $n_0^{-1/3}=9\times10^{-5}$ cm. We hence find that conditions (84) and (86) can be well satisfied with $\beta_m=8.3\times10^3\,\mathrm{cm}^{-1}$ and, using (87), $\omega=3.8\times10^{13}$ rad/s (wavelength $\lambda=50\,\mu$m). For $m=1$ this is attained with period $L\simeq9.5\,\mu$m.

We conclude that the theoretical limitations (84, 86) permit collective traveling wave interaction and possible traveling wave amplifiers and oscillators in the submillimeter wavelength regime [64]. With further increase in the electron beam density and the overcoming of technological difficulties in the fabrication and operation of extreme short period devices, it is theoretically conceivable that such devices can operate in the collective mode at the intermediate infrared frequency regime.

At shorter wavelengths, short periods and less dense electron beams, collective traveling wave interaction cannot take place, but amplifying devices operating on single-electron interaction principles (Secs. 2, 3) can still be constructed. The Smith-Purcell radiation [2] which operated at the visible wavelength regime with grating period $L=1.67\,\mu$m and electron density $n_0=7.4\times10^6\,\mathrm{cm}^{-3}$ belongs in this category. It is possible to verify that none of conditions (82) to (86) was satisfied in that experiment and hence that it is a single electron interaction effect.

6. Discussion on Some Free-Electron Lasers

An accelerated electron beam constitutes a situation of electronic population inversion. Therefore, in a periodic structure or slow wave structure where radiative transitions between free-electron states are permitted, it is possible to get either spontaneous emission or amplification by stimulated emission of radiation. If, in addition, a feedback mechanism is introduced into the device it is possible to get a free-electron laser oscillator [21, 70].

Many familiar electron beam devices and effects, like the traveling wave tube amplifier [1], the Smith-Purcell radiation [2], the Cerenkov radiation and bremsstrahlung provide either spontaneous or a stimulated emission of radiation, and in principle they all can be used to construct lasers and laser oscillators.

In the present section we wish to discuss some of these effects and the relations between them in view of the simplified model derived in the previous sections. This model is somewhat limited and not general enough to discuss accurately all the effects of interest, but it is good enough to describe and to explain their main features.

6.1. The Smith-Purcell Radiation

In the Smith-Purcell experiment spontaneous emission of visible light was observed from an optical grating when an electron beam traversed in close proximity to the grating and perpendicularly to the grating ruling direction [2].

This effect can be described in terms of the present model as interaction between the electron beam and an

evanescent Floquet space harmonic of a radiation mode in the vicinity of the grating. The situation is somewhat different from the case which we analyzed before, where interaction with a discrete electromagnetic mode was considered. In the Smith-Purcell experiment an open structure was used which supports a continuum of radiation modes. Of course, it is conceivable that the same experiment can be conducted in a confined structure (waveguide) where also efficient amplification of confined and discrete light modes by stimulated emission may be expected [21, 70]. In this case the coupled-mode single-electron-interaction analysis of Secs. 2 and 3 is well suited to describe the interaction.

The dispersion relation of the Smith-Purcell radiation was found to be [2]

$$m\lambda = L\left(\frac{c}{v_0} - \cos\theta\right), \tag{89}$$

where θ is the emission angle. This expression is consistent with the discussion in the previous sections, except for a small difference resulting from the fact that the experiment involved spontaneous emission while our analysis was mostly related to stimulated emission. We use in (89) the relation (10) $\beta_m = (2\pi/\lambda)\cos\theta + m2\pi/L$, where $\beta_0 = (2\pi/\lambda)\cos\theta$ is the z component of the propagation constant of a radiation mode propagating at an angle θ to the grating. This gives

$$v_0 = \frac{\omega}{\beta_m} = v_{ph_m}. \tag{90}$$

This is somewhat different from the previously derived Cerenkov condition (8), which requires inequality in (90). Indeed we should expect no stimulated emission gain exactly at the exact synchronism condition (90) because then the effects of stimulated emission and absorption are equal. Equations (26), (61), (65) and Fig. 9 suggest that maximum stimulated emission gain is expected around

$$\omega/\beta_m - v_0 \simeq v_{th} \tag{91}$$

instead of (90). Hence, instead of (89) the maximum gain condition is

$$m\lambda = L\left(\frac{c}{v_0 - v_{th}} - \cos\theta\right) \tag{92}$$

which usually is not much different from (89) since $v_{th} \ll v_0$.

Another feature of the Smith-Purcell effect which is consistent with the present analysis is the polarization of the emitted radiation. Like in the traveling wave tube amplifier, the electric field of the radiation must have a component along the longitudinal (z) direction (a TM mode), otherwise there will be no longitudinal coupling, see (19) and (1). This was actually confirmed in the original experiment [2].

An expression for the gain of Smith-Purcell free electron laser can be found right away from (26), (75)

$$\alpha = \frac{\varepsilon}{2\gamma_0^3} K_m S\omega k_D^2 \operatorname{Im}\{G'(\zeta_m)\}. \tag{93}$$

It is important at this point to notice that in our analysis we have assumed an infinite length of interaction and a perfect periodic structure. In practice the periodic structure of the electron beam will be of finite length l. This would mean that the momentum of the space harmonic $\beta_m = \beta_0 + 2\pi m/L$ will be defined to within an uncertainty of $\Delta\beta_m = 2\pi/l$. The uncertainty in the momentum due to the finite length or imperfection of the periodic structure leads to relaxation of the momentum conservation condition (11) so that transitions do not take place any more only between pairs of states with distinct longitudinal momentum (as shown in Fig. 1) but other electrons in the electron beam distribution will participate in the interaction. In the classical limit the uncertainty in momentum leads to uncertainty in ζ_m (65), which mean that electrons within range $\Delta\zeta_m = \omega(\beta_m^2 v_{th})^{-1}_{\Delta\beta_m}$ of the electron distribution $g(\zeta_m)$ participate in the interaction. We should require $\Delta\zeta_m \ll 1$ in order for our present analysis to apply. Since $\omega/\beta_m \approx v_0$ this condition can be written as

$$\frac{\Delta\beta_m}{\beta m} \ll \frac{v_{th}}{v_0}. \tag{94}$$

The regime defined by this inequality can be called "inhomogeneous broadening regime" and the opposite limit corresponds to homogeneous broadening. As in conventional laser theory, saturation in the laser gain may be reached in the first case by "burning holes" in the electron beam distribution function and depleting the population inversion between the states which take part in the transitions. In the homogeneous broadening case all the electrons in the beam participate in the interaction and hole burning does not occur. A similar distinction between the two regimes was also pointed out in reference to the Compton laser [26] and the bremsstrahlung laser [27]. In these examples the homogeneous broadening assumption is usually more realistic.

Within the limitations of inequality (94) and assuming a thin electron beam compare to the decay length of the electromagnetic space harmonic away from the periodic structure (grating), (93) is a useful first-order approximation to estimate the gain of a Smith-Purcell type free-electron laser. As would be expected for single-electron interaction the gain is proportional to the electron beam density n_0 (64). The dependence of the gain on the frequency ω is not obvious from (93)

since the interaction impedance K_m is usually dependent on ω and so is also the interaction cross section area S (keeping in mind that the width of the beam should be thinner than the decay length of the electromagnetic space harmonic away from the grating). Substitution of interaction impedance expressions which correspond to some practical structures [21] results in that at high frequencies the gain given by expression (93) is inversely proportional to the frequency ω and thus it would be hard to operate the Smith-Purcell laser at very short wavelengths.

6.2. The Cerenkov Radiation

The Cerenkov radiation effect is closely related to the Smith-Purcell radiation effect and to the discussion in this paper. It is different only in the fact that the "slow-wave structure" in this case is uniform matter (with index of refraction $n>1$) instead of a periodic structure. Like the Smith-Purcell radiation, the Cerenkov radiation is usually observed as spontaneous emission in open structures. However, electromagnetic wave amplification by stimulated Cerenkov emission in confined structures is possible [31, 32, 70]. In such structures the single electron interaction analysis (Secs. 2, 3) is well suited to describe the interaction in optical frequencies. Since the interaction in this case is with the whole longitudinal component of the electromagnetic wave, the interaction impedance (23) which should be used in (26) is approximately

$$K_0=\frac{1}{n}\sqrt{\frac{\mu}{\varepsilon_0}}\frac{\sin^2\theta}{\cos\theta}\frac{1}{\beta_0^2 S}, \tag{95}$$

where $\sqrt{\mu/\varepsilon_0}\simeq 377\,\Omega$ is the vacuum impedance and θ is the "zigzag" angle of the (TM) electromagnetic mode which propagates in the confined structure (waveguide). Equations (26), (75) and (95) result in an approximate expression for the gain in a Cerenkov waveguide laser

$$\alpha=\frac{k_D^2}{\gamma_0^3 nk}\frac{\sin^2\theta}{\cos^3\theta}\operatorname{Im}\left\{G'\left[\frac{c/(n\cos\theta)-v_0}{v_{th}}\right]\right\}. \tag{96}$$

Since $\operatorname{Im}\{G'(\zeta)\}$ has a maximum around $\zeta=-1$ (see Fig. 9), (96) suggests maximum gain at an angle

$$\cos\theta=\frac{c}{n(v_0-v_{th})}, \tag{97}$$

which is slightly different from the conventional expression for spontaneous Cerenkov radiation.

Equation (96) indicates that also the stimulated Cerenkov radiation gain is inversely proportional to the radiation frequency.

6.3. The Magnetic Bremsstrahlung Laser

The Stanford magnetic bremsstrahlung experiment [3, 14] is an example of a free-electron laser in which the periodic structure affects the electron beam only. It was discussed in the Introduction and distinguished from the Smith-Purcell mechanism for which we presented in the successive sections a quantitative analysis. This analysis does not apply to the bremsstrahlung type free-electron laser. However, since the kinematic of processes (b) and (c) of Figs. 2, 3 (describing the bremsstrahlung laser) is similar to that of process (a) (Smith-Purcell-Cerenkov laser), same gain condition is expected. Indeed Madey's radiation condition [3] (in the limit of small magnetic field)

$$\lambda\simeq\frac{L}{2\gamma^2} \tag{98}$$

can be shown to be equivalent to (90) ($m=1$) in the relativistic limit [21].

The "magnetic bremsstrahlung free-electron laser" is basically a single-electron interaction effect (since conditions (82) to (86) are not satisfied). This fact answers the question raised by Madey with regard to the difference between his calculated gain expression and the conventional traveling wave amplifier gain expression [14]. In a single-electron interaction the gain is proportional to the electron density (or current density), as obtained by Madey. By contrast, in the traveling wave tube the dependence of the gain on the electron density is more involved, and the first-order approximation, like (26), is not permitted because of the coupling to the longitudinal plasma wave. Instead the complete dispersion Eq. (24), or specifically (79) should be solved.

Of course, also *collective* interaction of an electron beam and an electromagnetic wave in a periodic *potential* structure are possible. It is demonstrated in the microwave frequency regime by the velocity jump amplifier [4] and the Ubitron [5, 31]. These devices can be regarded as other examples of bremsstrahlung free-electron lasers operating in the collective mode.

6.4. Interactions in the Crystal Lattice

The channeling of electrons in the crystal lattice provides us with examples of single-electron radiative emission effects which are similar to the free-electron laser effects and merit a short discussion on the basis of the presented models. Notice that also the electromagnetic wave with which the interaction takes place may be a "waveguided" mode in the x-ray regime (the Borrman effect [66]).

The effect of channeling radiation [8] was previously discussed in the Introduction and presented as an example of a transverse confining force free-electron

laser which is anelogous to the cyclotron resonance maser. Also the coherent bremsstrahlung effect was explained in Section 1. It is schematically described by diagrams (b) and (c) of Fig. 3 where the momentum G which is delivered to the electron wave either in the initial state (c) or in the final state (b) in order to balance the momentum conservation Eq. (4) is a vector of the crystal reciprocal lattice. It is suggested here that the process described by scheme (a) in Fig. 3 also exists in the crystal lattice, because the electromagnetic wave is effected by the crystal periodicity when propagating inside the crystal, in the same way that the electron waves are. This process may be regarded as "generalized coherent Cerenkov radiation". It should be distinguished from the conventional Cerenkov radiation effect which is independent on the periodicity of the crystal and depends only on the "average index of refraction" of the material $-n$. In the x-ray regime $n<1$ and therefore there is no conventional Cerenkov radiation.

To find the contribution of process (a) to the interaction of electrons with electromagnetic waves in the crystal lattice, one must first obtain the Floquet mode solution of the electromagnetic wave in the crystal

$$E(r,t)=\sum_G E_G(q,\omega)e^{i(q_G\cdot r-\omega t)} \tag{99}$$

$$q_G=q+G, \tag{100}$$

where G is a reciprocal lattice vector. The space harmonic amplitude E_G is calculated from the infinite set of equations

$$q_G\times q_G\times E_G(q,\omega)=-\omega^2\mu\sum_{G'}\varepsilon_{G,G'}(q,\omega)E_{G'}(q,\omega) \tag{101}$$

which results from Maxwell equations. The dielectric matrix elements $\varepsilon_{G,G'}$ were defined by Adler and Wiser [67].

Equations (101) can be readily solved by some simplifying approximation [68, 71]. The solution shows that the amplitude of the longitudinal components $(E_G\cdot G/|G|)$ of the space harmonics may be non negligible compare to the fundamental space harmonic. In a simple minded model one may use the calculation of the space harmonic amplitudes to find the interaction impedance (23) and the gain (26) using the same model we used for the Smith-Purcell free-electron laser. It is apparent that this would be too crude a description of the problem since a more general relativistic quantum mechanical analysis should be used and homogeneous laser broadening should be assumed. However, the indication of the simplified model that the "coherent Cerenkov radiation" gain reduces appreciably at short wavelengths is probabely correct and conforms with prediction and measurements of very weak interactions in the x-ray and γ-ray frequency regimes with coherent bremsstrahlung [57] and stimulated Compton effect [50]. By contrast, quite strong x-ray and shorter wave length radiation is predicted for the channeling radiation effect [9] making it more attractive for possible future coherent x-ray radiation.

7. Conclusion

The interaction of an electron beam with electromagnetic waves was discussed in terms of a simple general model. Collective and single-electron interactions were distinguished as two different regimes of operation, which can take place under different conditions. We also distinguish between three classes of interactions (a) The radiative electronic transitions are made possible in a (periodic) structure which increases the momentum of the electromagnetic field so that momentum can be conserved in the process (Cerenkov-Smith-Purcell class). (b) The missing longitudinal momentum is provided to the electrons (bremsstrahlung class). (c) The radiative transitions are made possible by a transverse confining force which is exerted on the electrons.

A simple "one-dimensional" coupled mode analysis was presented, providing expressions for free-electron laser gain and gain conditions in the classical, quantum-mechanical and also degenerate plasma regimes. For some applications the validity of the analysis is limited and some further elaboration of the model would be necessary. This includes an accounting for transverse electromagnetic field components and transverse field variation (which is necessary when the electron beamwidth is not negligible), situations where the interaction is not with a discrete single electromagnetic mode but with continuum of modes, and situations in which the interaction length is a limiting factor. In the last mentioned case, which is often the practical case and also when the accuracy of the periodic structure is finite, the momentum conservation condition (4) needs not be satisfied exactly and thus different (homogeneous broadening) analysis should be used.

The present discussion suggests that a number of useful free-electron lasers based on principles of Cerenkov, Smith-Purcell and bremsstrahlung radiation may be constructed. The operation frequency can be determined by an appropriate choice of the period of the periodic structure and by varying the electron beam energy. This last possibility also provides the advantage of laser tuning. Other foreseeable advantages of free-electron lasers are possible high power operation and high efficiency (with storage ring [3] or with decelerating electron collector electrode [70]), and the potential for coherent laser sources from the far infrared to possibly the short U.V. regime.

Appendix

In the appendix we show that (84), (86) are equivalent to requiring that the space charge wave bunching energy exceed the thermal energy and the mean Coulomb repulsion energy between individual electrons[3].

The energy stored in one bunched period per unit beam area is Q^2/C where $Q = en_0 2\pi/\beta$ is the charge (per unit area) in one bunched period $2\pi/\beta$, and $C = \varepsilon\beta/2\pi$ is the capacitance per unit area of one period. The average collective energy per electron is then found to be

$$\mathscr{E}_{\text{collect}} = \frac{n_0 e^2}{\varepsilon}\left(\frac{2\pi}{\beta}\right)^2. \tag{A.1}$$

The average thermal energy per electron is

$$\mathscr{E}_{\text{thermal}} = k_B T. \tag{A.2}$$

The Coulomb repulsion energy between individual electrons is

$$\mathscr{E}_{\text{coulomb}} = \frac{1}{\varepsilon}\frac{e^2}{n_0^{-1/3}}, \tag{A.3}$$

where $n_0^{-1/3}$ is the average distance between electrons.

Equation (84) is readily derived by requiring that (A.1) is much larger than (A.2), using definition (64). Equation (86) is derived from the requirement that (A.1) is much larger than (A.3).

Acknowledgements. We wish to thank Prof. R. Feynman, Prof. A. Rose and Prof. S. L. Schlesinger for helpful discussions.

References

1. J.R.Pierce: *Traveling Wave Tubes* (Van Nostrand, Princeton 1950)
2. S.J.Smith, E.M.Purcell: Phys. Rev. **92**, 1069 (1953)
3. L.Elias, W.Fairbank, J.Madey, H.A.Schwettman, T.Smith: Phys. Rev. Lett. **33**, 717 (1976)
4. L.M.Field, P.K.Tien, D.A.Watkins: Proc IRE **39**, 194 (1951)
5. R.M.Phillips: IRE Trans. ED-**7**, 231 (1960)
6. J.Schneider: Phys. Rev. Lett. **2**, 504 (1959)
7. L.Landau: Z. Physik **64**, 629 (1930)
8. M.A.Kumakhov: Phys. Lett. **57**, 17 (1976)
9. R.W.Terhune, R.H.Pantell: Appl. Phys. Lett. **30**, 265 (1977)
10. J.V.Jelley: *Cerenkov Radiation and its Applications* (Pergamon, New York 1958)
11. J.D.Jackson: *Classical Electrodynamics* (J. Wiley, New York 1962)
12. M.A.Piestrup, R.H.Pantell, H.E.Puthoff, G.B.Rothbart: J. Appl. Phys. **44**, 5160 (1973)
13. D.Marcuse: Bell Syst. Tech. J. **41**, 1557 (1962); ibid **42**, 415 (1963)
14. J.M.Madey: J. Appl. Phys. **42**, 1906 (1971)
15. D.Coleman, C.Enderby: J. Appl. Phys. **31**, 1695 (1960)
16. W.Stroke: In *Handbuch der Physik*, Vol. XXIX, ed. by S. Flugge (Springer Berlin, Heidelberg, New York 1967) p. 440
17. Historical Notes, IEEE Trans.—special issue, ED-**23**, 714—738 (1976)
18. J.W.Gewartovski, H.A.Watson: *Principles of Electron Tubes* (Van Nostrand, Prjnceton 1965)
19. V.L.Ginzburg, V.Zheleznyakov: Phil. Mag. **11**, 197 (1965)
20. I.Palocz, A.A.Oliner: Proc. IEEE **53**, 24 (1965); and **55**, 46 (1967)
21. A.Gover: "Wave Interactions in Periodic Structures and Periodic Dielectric Waveguides"; Caltech report (Feb. 1976)
22. K.Mizuno, S.Ono: J. Appl. Phys. **46**, 1849 (1975)
23. K.Mizuno, Y.Shibata: IEEE Trans. ED-**20**, 749 (1973)
24. R.H.Pantell: *Symposium on Millimeter Waves* (Polytechnic Institute of Brooklyn, 1959) p. 301
25. R.B.Palmer: J. Appl. Phys. **43**, 3014 (1972)
26. V.P.Sukhatme, P.A.Wolff: J. Appl. Phys. **44**, 2331 (1973)
27. F.A.Hopf, P.Meystre, M.O.Scully, W.H.Louisell: Phys. Rev. Lett. **37**, 1215 (1976)
28. S.E.Graybill, S.A.Nablo: IEEE Trans. NS-**14**, 782 (1967)
29. J.A.Nation: Appl. Phys. Lett. **17**, 491 (1970)
30. N.F.Kovalev, M.I.Petelin, M.D.Raizer, A.V.Smorgonskii, L.E.Tsopp: ZhETF Pis. Red. **18**, 232 (1973)
31. J.E.Walsh, T.C.Marshal, S.P.Schlesinger: Phys. Fluids **20**, 709 (1977)
32. H.Lashinsky: In *Advances in Electronics and Electron Physics*, ed. by L. Marton (Academic Press, New York 1961) p. 265
33. F.Friedman, M.Herndon: Phys. Rev. Lett. **28**, 210 (1972)
34. P.C.Efthimion, S.P.Schlesinger: Phys. Rev. A. **16**, 633 (1977)
35. W.Manheimer, E.Ott: Phys. Fluids **17**, 463 (1974)
36. J.L.Hirshfield, J.M.Wachtel: Phys. Rev. Lett. **12**, 533 (1964)
37. I.B.Bott: Phys. Lett. **14**, 293 (1965)
38. D.V.Kisel, G.S.Korablev, V.G.Navelyev, M.I.Petelin, Sh.Ye.Tsimring: Sov. Radio Eng. and Elect. Phys. **19**, 95 (1974)
39. N.I.Zaytsev, T.B.Pankratova, M.I.Petelin, V.Flyagin: Sov. Radio Eng. and Elect. Phys. **19**, 103 (1974)
40. M.Friedman, D.A.Hammer, W.M.Manheimer, P.Sprangle: Phys. Rev. Lett. **31**, 752 (1973)
41. V.L.Granatstein, M.Herndon, R.K.Parker, P.Sprangle: IEEE J. QE-**10**, 651 (1974)
42. V.L.Granatstein, M.Herndon, P.Sprangle, Y.Carmel, J.S.Nation: Plasma Phys. **17**, 23 (1975)
43. M.Friedman, M.Herndon: Appl. Phys. Lett. **22**, 658 (1973)
44. V.L.Granatstein, M.Herndon, R.K.Parker, S.D.Schlesinger: IEEE Trans. MTT-**22**, 1000 (1974)
45. V.L.Granatstein, S.P.Schlesinger, M.Herndon, R.K.Parker, J.A.Passour: Appl. Phys. Lett. **30**, 384 (1977)
46. P.Sprangle, V.L.Granatstein, L.Baker: Phys. Rev. A **12**, 1697 (1975)
47. P.Sprangle, V.L.Granatstein: Appl. Phys. Lett. **25**, 377 (1974)
48. R.H.Pantell, G.Soncini, H.Puthoff: IEEE J. QE-**4**, 905 (1968)
49. V.A.Dubrovskii, N.B.Lerner, B.G.Tsikin: Sov. J. Quant. Electron. **5**, 1248 (1975)
50. A.Hasegawa, K.Mima: Appl. Phys. Lett. **29**, 542 (1976)
51. V.P.Sukhatme, P.A.Wolff: IEEE J. QE-**10**, 870 (1974)
52. H.Uberall: Phys. Rev. **103**, 1055 (1956)
53. V.A.Belyakov: JETP Lett. **13**, 179 (1971)
54. V.V.Batygin: Phys. Lett. **28A**, 65 (1968)
55. G.Diambini Palazzi: Rev. Mod. Phys. **40**, 611 (1968)
56. R.L.Walker, B.L.Berman, R.C.Der, T.M.Kavanagh, J.M.Khan: Phys. Rev. Lett. **25**, 5 (1970)
57. R.L.Walker, B.L.Berman, S.D.Bloom: Phys. Rev. A **11**, 736 (1975)
58. R.Tsu, L.Esaki: Appl. Phys. Lett. **22**, 562 (1973)
59. J.Lindhard: Kgl. Danske Viden Skab. Selskab. Mat. Fys. Medd. **28**, #8 (1954)
60. B.D.Fried, S.D.Conte: *The Plasma Dispersion Function* (Academic Press, New York 1971)
61. L.Landau: J. Phys. USSR **10**, 25 (1946)
62. A.Gover, H.K.Burrell, A.Yariv: J. Appl. Phys. **45**, 4847 (1974)
63. A.H.Poritsky: IRE Trans. PGED-2, 60 (1953)
64. A.Yariv, D.Armstrong: J. Appl. Phys. **44**, 1664 (1973)
65. I.Palocz, A.A.Oliver: *Symp. Quasi-Optics* Polytechnic Inst. of Brooklyn (1964) p. 217
66. B.W.Batterman: Rev. Mod. Phys. **36**, 681 (1964)
67. L.Adler: Phys. Rev. **126**, 413 (1962); N.Wiser: Phys. Rev. **129**, 62 (1963)
68. D.L.Johnson: Phys. Rev. **B12**, 3428 (1975)
69. A.Gover, A.Yariv: J. Appl. Phys. **46**, 3946 (1975)
70. A.Gover, A.Yariv, P.Yeh: VIII Internat'l. Quantum Electronics Conf. Abstract; see Optics Commun. **18**, 222 (1976)
71. A.Gover: Calculation of longitudinal components, unpublished. See also [21]
72. D.A.G.Deacon, L.R.Elias, J.M.J.Madey, G.J.Ramian, H.A.Schwettman, T.I.Smith: Phys. Rev. Lett. **38**, 892 (1977)

[3] We acknowledge Prof. Albert Rose for contributing this interpretation